JOURNAL OF OPTOELECTRONICS AND ADVANCED MATERIALS Vol. 17, No. 5-6, May – June 2015, p. 691 - 698

pH effect on physical properties of zinc oxide nano structures grown by sol- gel

H. R. ALAEI[a*], M. YUONESI[b]
[a]*Department of Physics,Varamin Branch, Islamic Azad University, Varamin, Iran.*
[b]*Department of Physics, Ayatollah Amoli Branch, Islamic Azad University, Amol, Iran.*

Using sol gel method, samples were grown and with changing the amount of precursor, pH of solvent was controlled. Thus, four samples were produced with the different pH. Atomic force microscopy (AFM), energy-dispersive X-ray (EDX) analysis and x-ray diffraction (XRD) structural characterization were performed on samples which showed smooth surface with zinc oxide structure. Transmittance (drying and annealing) and photoluminescence spectra and also band gap calculations showed that optical property depends on pH of solvent. Magnetic property of samples was done by magnetic force microscopy (MFM) and quantum design. Results show that the magnetic property may depend on changing of pH of solvent.

(Received October 27, 2014; accepted May 7, 2015)

Keyword: Sol gel, EDX, XRD, AFM, MFM, Zinc oxide

1. Introduction

Transparent conducting oxides (TCOs) have longly been a subject of various investigations due to their unique physical properties and applications in commercial devices. Among TCOs, ZnO is one of the most promising materials for the fabrication of the next generations of optoelectronic devices in the UV optical region and or display devices. The physical properties of zinc oxide strongly depend on method and type of growth. There are the various methods of growth such as sputtering, metal organic chemical vapor deposition (MOCVD), vapor transport, pulsed laser deposition (PLD), spray pyrolysis, molecular beam epitaxy (MBE), isothermal sintering, chemical vapor deposition (CVD), electrochemical deposition, hydrothermal method and etc [1-5]. Another method based on chemical method for the production of ZnO thin films is sol-gel which is widely used in the synthesis of ZnO nano crystals. The sol-gel process is simple, inexpensive in fabrication, to produce a large number of samples, easier composition control and the accurately controlled mole ratio, the high solubility, better homogeneity, lower processing temperature and has a general advantage for large area deposition and thickness of the films. There are many environment parameters for controlling the growth of a crystal. Dip, spary and spin coatings are three recognized ways at the sol gel technique. In this paper, using the spin sol–gel technique, four films with four types of ZnO solvent at different pH of solvent were grown and then the structural, optical and magnetic properties of the grown films were investigated.

Kind of crystal (bulk, quantum wire and dot, thin film or powder) and environmental conditions such as temperature, pressure, humidity and doping concentration are other factors which change the physical properties of zinc oxide semiconductor. Here, zinc oxide nano films were grown on glass substrate for studying pH effects. The produced films by sol – gel method are commonly grain or fiber forms but how their size are controlled, are still an important problem. This work can be a good answer for it that is reported first time.

Owing to unique physical properties, it has many applications in industry such as gas sensors, surface acoustic devices, transparent electrodes, solar cells, photodetectors, light-emitting diodes and lasers and etcetera. The done works in this paper can improve the physical properties of zinc oxide and the yield of the extant equipments can be increased consequently [6-8]. This paper shows that the acidic solvents ($pH<7$) how changes physical properties of zinc oxide but the pH effect for alkaline solvent ($pH>7$) has been investigated previously [9].

2. Experimental method

ZnO nanofilms were prepared by the sol–gel method. In this experimental work, three stages have been used that they are preparation of materials, synthesis and characterization techniques. Every section will be explained.

2.1 Preparation of materials

The utilized precursors for the synthesis of ZnO nanofilms are: zinc acetate dehydrate [$Zn(CH_3COO)_2$-$2H_2O$], 2-mithoxyethanol (DME) [$C_3H_8O_2$] and monoethanolamine (MEA) [C_2H_7NO] used as zinc source, solvent and stabilizer, respectively.

2.2 Syntheses

Four samples of ZnO nanofilms were prepared by the spin sol–gel method. In the beginning, zinc acetate was dissolved in a mixture of DME and MEA solution at room temperature. For the change of acidic environment, the molar ratio of MEA to Zn was maintained at 0.5, 1, 1.5, 2. At 80 ^{o}C, solutions were vigorously stirred for 1h by means of a magnetic stirrer to yield a clear and homogeneous solution. At room temperature, the solutions were aged at least for 24h to obtain the desirable sol and then they were deposited by the spin coating technique on the glass slide substrates which were beforehand cleaned. The solution was dropped onto the glass slide substrates, which were rotated at 3000 rpm for 30s. After depositing by spin coating, the nanofilms were dried at 200 ^{o}C for 20 min to evaporate the solvent and remove organic residuals. This procedure, from depositing to drying, was repeated four times to reaching the desired thickness. In an open air furnace, the nanofilms were finally heated at 500 ^{o}C for 1h. The samples for characterization techniques became cold slowly until reaching to room temperature.

2.3 Characterization techniques

The coated nanofilms were characterized to study the optical and structural properties. The selected pH matter is Jenway 35.5 model. The compositional analysis was carried out by energy-dispersive X-ray (EDX) analysis (JEOL JSM 6300 Oxford-7582). The x-ray diffractometer (XRD6000, Shimadzu, Japan) with a CuK$_{\alpha}$ radiation line (1.5406 ˚A) was used for crystalline phase and to determine the orientation of nanofilms. The room temperature optical transmittance was measured by a UV–Vis spectrophotometer (Varian Cary). Room temperature photoluminescence (PL) measurement was performed with using HR800 LabRam Infinity Spectrophotometer excited by a continuous He–Cd laser with a wavelength of 325 nm at a power of 50 mW. Nanosurf model atomic force microscope (AFM) and magnetic force microscope (MFM) were used to study the magnetic and structural surface morphology of nano films. The magnetic properties of the samples in the room temperature were measured using Quantum Design MPMS-7.

3. Results and discussion

3.1 pH

The produced solvent can be acidic, neutral and alkaline media that can affect on physical properties of samples. For the change of acidic environment (pH), the molar ratio of MEA to Zn was changed. Table 1 shows pH of solvents which are 4.7, 5.6, 6.1 and 6.8 for samples 1, 2, 3 and 4. Chemistry behind this change and the reaction involved can be written as below:

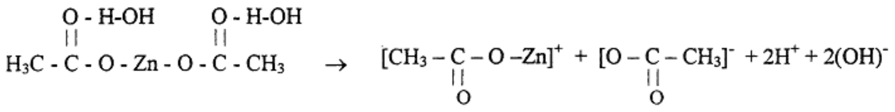

$$\mathrm{H_3C-\overset{\overset{O-H\text{-}OH}{\|}}{C}-O-Zn-O-\overset{\overset{O-H\text{-}OH}{\|}}{C}-CH_3} \rightarrow [\mathrm{CH_3-\underset{\underset{O}{\|}}{C}-O-Zn}]^+ + [\mathrm{O-\underset{\underset{O}{\|}}{C}-CH_3}]^- + 2H^+ + 2(OH)^-$$

Table 1. The physical details for the annealed samples

sample	pH	Lattice constant (A^{o})				TC (101)	FWHM(^{o}) (101)	Grain size (nm)	Roughness average (nm)	FWHM for PL (nm)	Band gap (eV)
		a=b		c							
		bulk	This worh	bulk	This work						
1	4.7	3.25	3.24951	5.2069	5.20662	2.79	0.475	8.25	3.67	15.3	3.285
2	5.6		3.24973		5.20673	2.82	0.345	13.81	5.13	16.5	3.258
3	6.1		3.24981		5.20681	2.86	0.325	18.73	7.76	17.9	3.249
4	6.8		3.24994		5.20688	2.89	0.305	24.32	9.12	18.1	3.242

The formation of zinc monoacetate is supposed to take place in the solution and when the glass substrate is heated, hydrolysis takes place producing acetic acid as reaction between

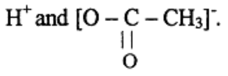

$$H^+ \text{ and } [\mathrm{O-\underset{\underset{O}{\|}}{C}-CH_3}]^-.$$

Zinc monoacetate which is formed in the above mentioned reaction is hydrolyzed by the following reaction:

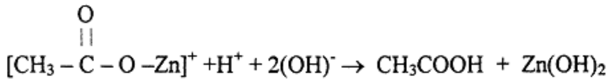

$$[\mathrm{CH_3-\overset{\overset{O}{\|}}{C}-O-Zn}]^+ + H^+ + 2(OH)^- \rightarrow \mathrm{CH_3COOH} + \mathrm{Zn(OH)_2}$$

ZnO is next formed by the chemical reaction:

$$\mathrm{Zn(OH)_2} \rightarrow \mathrm{ZnO} + \mathrm{H_2O}$$

A colloid is a suspension in which the dispersed phase is so small from 1 to 1000 nm. A sol is a colloidal suspension of solid particles in a liquid. All of these types of colloids can be used to generate polymers or particles from which ceramic materials can be made. Changing of the molar ratio MEA to Zn is caused that the colloid size modified. This change alters the band gap. Perhaps, this is chemistry behind these changes.

3.2. Structural properties

3.2.1 EDX

For knowing and assuring the structures of zinc oxide, we performed EDX for sample 1. EDX analysis illustrated in fig. 1 for sample 1 shows that Zn and O elements in the starting solution present in the solid film. The Si elements that are not expected to be in solid films may be probably a result from the glass substrates. The ratio of elemental weights (wt.%) of Zn and O elements in the ZnO nano film is 0.94. This spectrum shows that the expected elements exist in the solid films.

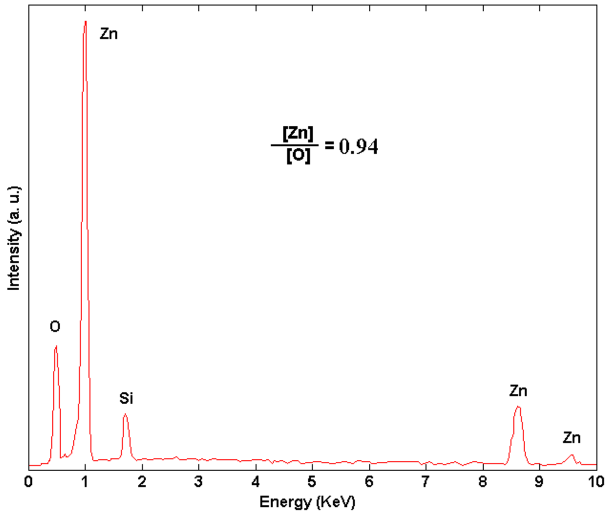

Fig. 1: EDX analysis for sample 1 shows that Zn and O elements in the starting solution present in the solid film.

3.2.2 XRD studies

Fig. 2 shows the XRD spectrum in the room temperature for all the annealed samples as a function of 2θ, which is changed from 30° to 70° with step 0.02°. The spectra of each sample correspond to the hexagonal wurtzite structure of zinc oxide without none of the preferred orientation along plane (0 0 2) or the other planes. As seen, the crystalline quality is decreased with decreasing the grain size of the samples. Because a material becomes the faraway form of bulky state, its surface atoms are absorbed toward the inner atoms of material by inter-atomic forces. This phenomenon causes that not only the grain size is condensed but also the order and regularity of planes in the various directions are ruined and consequently, the XRD spectrum is dispersed. Perhaps, the reduction of the lattice constant, as seen in table (1), with reducing the grain size refers to this reason. The preferred orientation of the ZnO nano films was evaluated by the texture coefficient (TC), calculated from the equation in following

$$TC^i = \frac{\dfrac{I_i}{I_o^i}}{\dfrac{1}{n}\sum_j^n \dfrac{I_j}{I_o^j}} \tag{1}$$

Where TC^i, I_i and I_o^i are the texture coefficient, observed (measured) peak intensity and standard peak intensity of powder from a material for i^{th} plane in (hkl) direction respectively. n is also the number of reflection planes. Deviation from unity implies the preferred growth. The calculations of TC show that the most abundant orientation of the growth is at the (101) direction. As seen in table (1), TC (the abundance of being crystallized) decreases with the decrease of grain size.

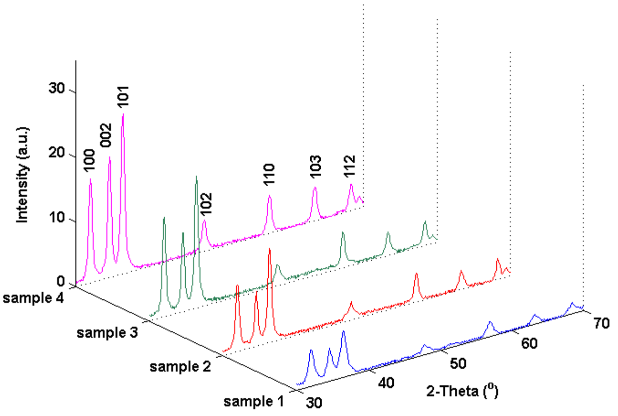

Fig. 2: XRD spectrum in room temperature for all annealed samples.

The average grain size of the ZnO nano film was estimated from X-ray diffraction using Scherer's formula

$$\text{grain Size} = \frac{k\lambda}{\beta\cos\theta} \tag{2}$$

Where, λ (1.5406 A°), θ, k (≈0.9) and β are the wavelength of the X-ray, the Bragg diffraction angle, Scherrer's constant and the full width half maximum (FWHM) of the peak at the XRD spectrum. For calculation of the grain sizes, the direction (101) was used because its TC is the bigger amount. As seen at table (1), the grain size of samples is between 8 until 25 nm. Thus, one of physical parameters that pH of the solvent changes is grain sizes of nanostructure zinc oxide.

3.2.3 Surface morphology

The AFM (Atomic Force Microscopy) is one way for showing the surface morphology of nano films. During AFM, the tip is scanned at a defined distance above the sample and hence the measurement mode is noncontact. Fig. 3 shows the AFM images of the annealed ZnO nano films with the various pH at the room temperature. For the correct collation, the scanned area and the seen height of all samples are the same and are equal 1μm × 1μm and 48.6 nm, respectively. All images illustrate the 3D topography of the nano films which were fitted by linear fit model. AFM results indicated that the surfaces of the grown nano films were relatively smooth. One of the qualitative parameters of the surface is the surface roughness which generally depends on annealing temperature. The annealing temperature can also affect the grain size of nano films. The root mean square (*RMS*) of roughness values for the samples is in Table 1 that it was calculated of the following relation.

$$RMS = \sqrt{\frac{1}{MN}\sum_{k=0}^{M-1}\sum_{l-0}^{N-1}\left(z\left(x_k, y_l\right)\right)^2} \qquad (3)$$

Where, RMS and $z\left(x_k, y_l\right)$ are the root mean square and the height of the scanned points, respectively. M and N are the number of the scanned points. The root mean square roughness of the samples is increased from 3.67 to 9.12 nm as pH of solvents is increased from 4.7 to 6.8. As seen, the root mean square roughness has a directly relation with pH. The smaller RMS is, the less pH will be that it has a directly relation with grain size.

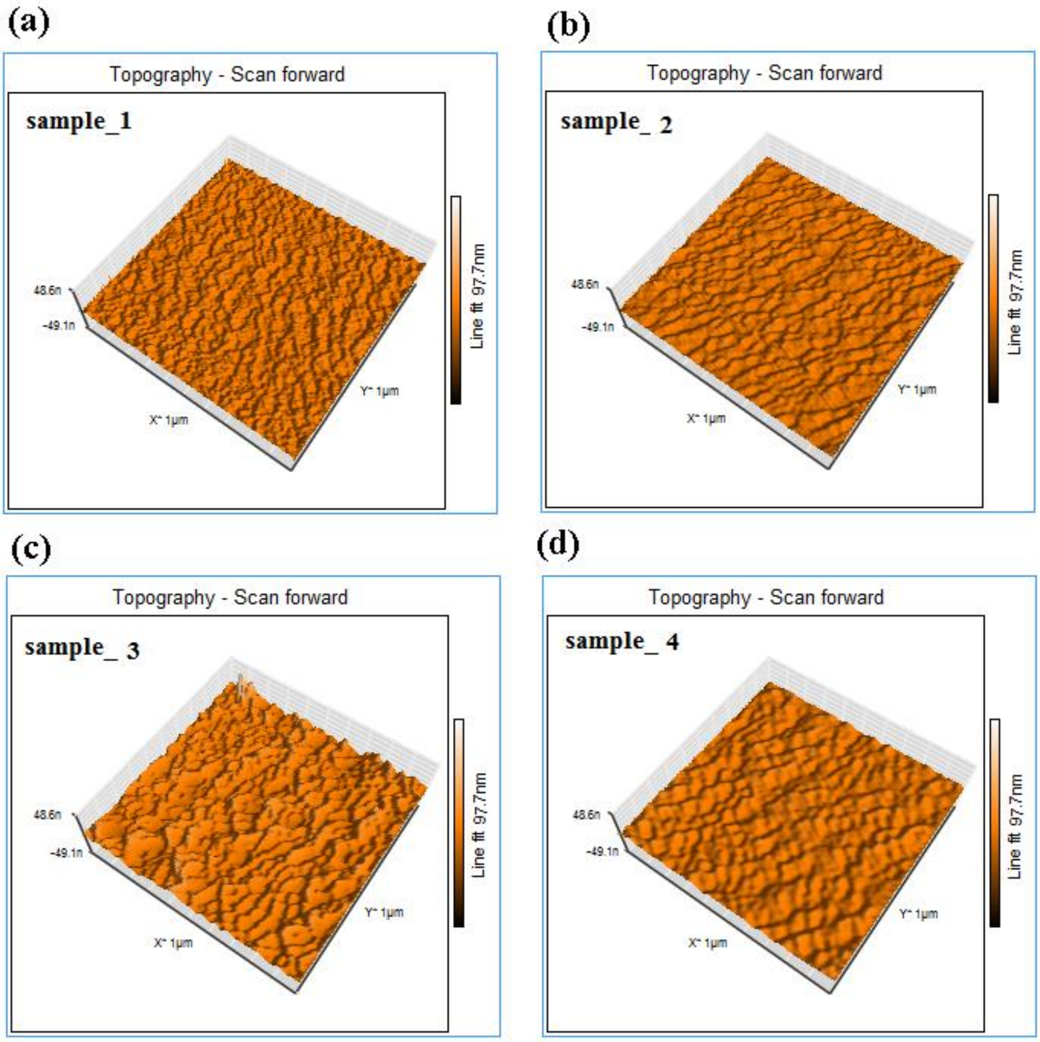

Fig. 3. The AFM images of the annealed ZnO nano films with various grain sizes in room temperature.

3.3. Optical properties

3.3.1 Transmittance spectrum

There are UV-Vis-IR areas in the transmittance spectrum from 200 to 800 nm. Figs. 3 and 4 illustrate the transmittance spectrum of the drying and annealing samples in the room temperature, respectively. The incident light, which is not absorbed or not refracted, forms the transmittance spectrum. For the drying temperature, the changes in the transmittance spectrum at the visible and infra red areas are almost 90% but are strongly decreased for ultra violet area. Because of the nonexistence of a perfectly crystalline structure and the existence of a gel structure, the surfaces of the deposited film layers are parallel and form an interference pattern. This interference pattern is more for the sample 4. The annealing temperature not only destroys the interferential pattern but also decreases the transmittance spectrum. The annealing temperature evaporates all organic materials and also gives an opportunity to the zinc oxide crystal structure to move their atoms and make a more arranged crystal form. Whatever ph becomes smaller, the transmittance spectrum is also decreased and it is a natural phenomenon due to the smaller grain size. Because of being decreased the grain size, the number of grains is increased at volume unit. The increase of grains at the volume unit causes increase interfaces at the volume unit. The interfaces cause to scatter the incident light and thus the transmittance spectrum is decreased. As Fig. 5 illustrates, the incident light is forcefully absorbed at the ultra violet area. This absorption is an electronic absorption that forms a band gap.

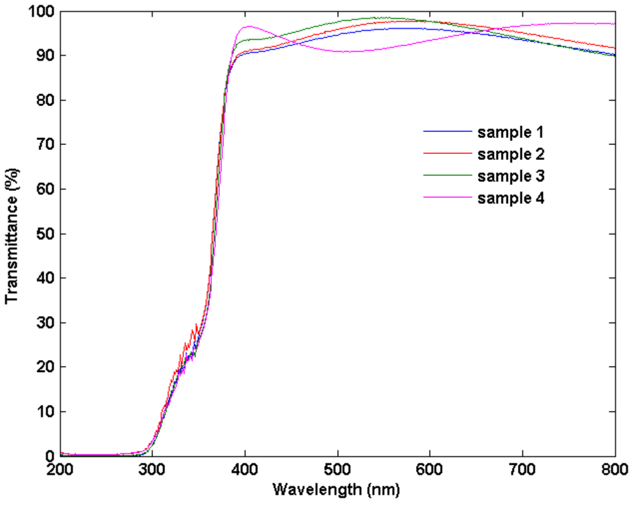

Fig. 4. The transmittance spectrum of the drying samples in room temperature.

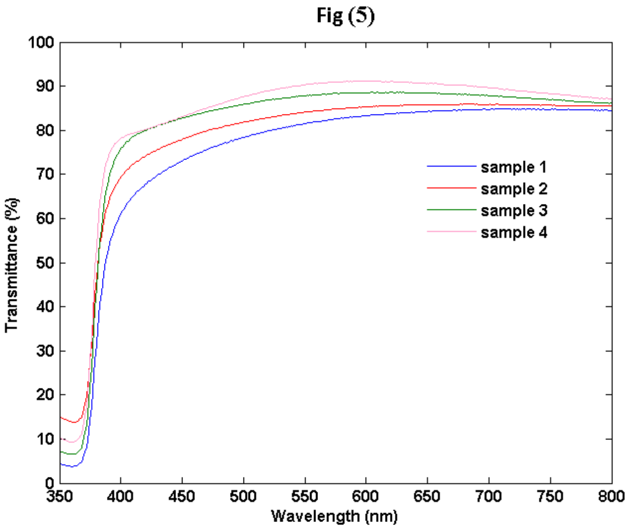

Fig. 5: The transmittance spectrum of the annealing samples in room temperature.

3.3.2 Band gap

Zinc oxide is a semiconductor with the direct band gap. The quantum theory of the direct optical absorption of materials gives the relationship between the absorption coefficient (α) and the photon energy of the incident light $(\hbar\gamma)$ as following

$$(\alpha\hbar\gamma)^2 = \hbar\gamma - E_g \quad (4)$$

The direct band gap is determined by fitting this equation with a straight line at $\alpha = 0$ by extrapolation. Fig. 6 shows $(\alpha\hbar\gamma)^2$ vs. the photon energy of the incident light for all samples. It can be mentioned that there are many environmental factors which affect on the band gap such as heat, dopant (Vegard's law), thickness of nano films, pressure, Moss–Burstein effect, pH of solvent and etc. Here, it is supposed that all conditions are the same with the exception of pH of solvent or it has the most effect. As Fig. 6 is indicating, the band gap is subtracted with increasing pH. It maybe refers to grain size that has been demonstrated at the insert picture of Fig. 6. The figure is the exhibition of the band gap energy versus the grain size. The difference of the band gap energy between samples 1and 2 (0.027) with samples 3 and 4 (0.007) shows that the smaller the grain size are, the bigger the changes of the band gap energy will be. This effect is completely a phenomenon of quantum mechanics. Suppose that each grain is spherical form with radius a, and has a weak interaction one another that we can thus relinquish it. Using Schrödinger's basic differential equation for the isolated grain; the whole of the band gap energy (E_g) for the material can be written with

$$E_g = E_{bulk} + \Delta E_{QCF} \quad (5)$$

$$\Delta E_{QCF} = E_{\min}^{el} + E_{\min}^{hole} = \left(\frac{\pi^2\hbar^2}{2}\right)\left(\frac{1}{m_e}+\frac{1}{m_h}\right)\left(\frac{1}{a^2}\right) \quad (6)$$

E_{bulk} is the bulk energy due to the periodic potential of the atoms of the material but ΔE_{QCF} is the energy changes due to the quantum confinement effect (QCF) in grains. As seen of relations (5) and (6), whatever the smaller the grain size is, the bigger the band gap energy will be that it is exactly coincidence with our experimental results.

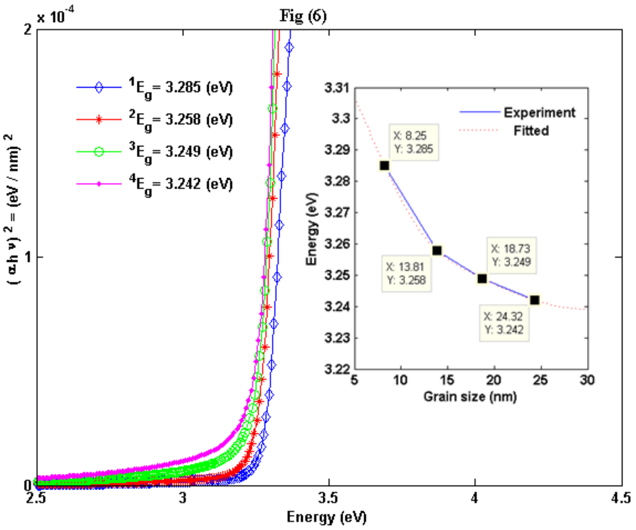

Fig. 6: the $(\alpha\hbar\gamma)^2$ vs. photon energy of incident light for all samples. The insert picture is the exhibition of the band gap energy versus the grain size.

3.3.3 Photoluminescence

Fig. 7 shows the photoluminescence spectrum of all samples in intervals 300 until 800 nm at the room temperature. The peak position illustrates photoluminescence type. Because the peak position is approximately near the band edge of the energy gap, it shows that the type of the recombination mechanism is free exciton (FE). We calculated band gap of samples with formula $(\alpha\hbar\gamma)^2 = \hbar\gamma - E_g$. Results of this calculation have been rewritten in table (1). As we know, excitation above the band gap generates free electrons and holes. This excition is a hydrogen-like state due to the coulomb interaction between an electron and a hole. The energy of a Free is slightly lower than the band gap. The peak positions have blue shift when pH of the solvents is diminished that it agrees very well with the calculations of the energy gaps due to grain size of samples. It refers to the quantum confinement effect in nano scales. Monochromatic light of each photo luminescence spectrum has a narrow width line that it shows its quality. For this reason, the full width half maximum (FWHM) of all spectra was calculated and table 1 shows it. As seen, FWHM is decreased with being decreased pH of the solvents and the light emission is also shifted to monochromatic light. There are radiative and nonradiative recombinations in each material. The nonradioactive recombinations produce heat in materials and its temperature is increased. One of factors, which decrease the intensity of the photoluminescence spectrum and spread the spectrum, is heat. To obtain a clear spectrum, without thermal excitation and broadening, the samples must be cooled because it decreases the phonon scattering.

As seen of Fig. 7, the intensity of the photoluminescence spectrum is subtracted with increasing pH of the solvents. Probability, all of these phenomena refer to grain size. We have not observed any visible emission for the sol gel nano films. It may refer to the factors of creation of these green emissions that are not the present in nano films. These factors are generally the surface-located complex emission, intrinsic defects at the surface, higher surface-to-volume ratio of the thin film, the oxygen or zinc vacancy, doping and etcetera. If the factors of creation of these green emissions are not present in film, we will not see the green emissions [10-13].

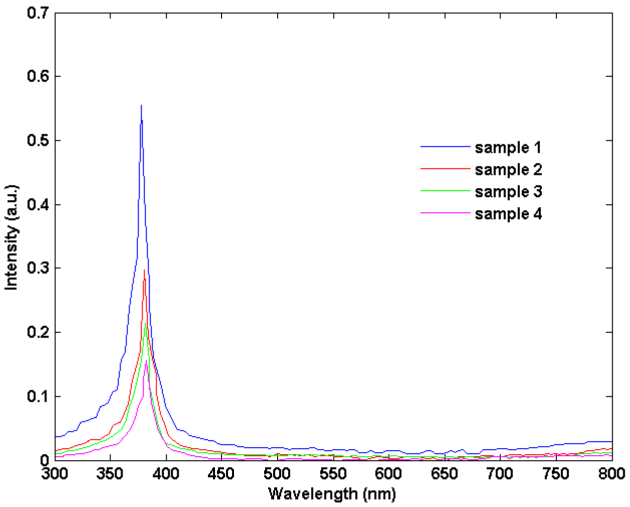

Fig. 7. The photoluminescence spectrum of all samples in intervals 300 until 800 nm at the room temperature.

3.3.4 Extinction coefficient

Fig. 8 shows the dependence of the extinction coefficient of the nanofilms on the wavelength. The optical constants of the nanofilms have been calculated by using pointwise unconstrained minimization algorithm and fitting the data to the Cauchy formula in thin films[14]. It is changed between 0.01 and 0.25 and also is constant in the long wavelength but in the vicinity of absorption edge it decreases the most amounts. The source k (absorption) refers to the inelastic scattering of the electromagnetic waves in the semiconductor such as the Compton effect, photoelectric effect, pair production effect and so on. Because our samples are magnetic, magnetic vector of incident light is absorbed or scattered more than the electrical vector in material. The peak of extinction coefficient of all samples has an anomalous behavior with variation of solvent pH that it refers to energetic absorption edge.

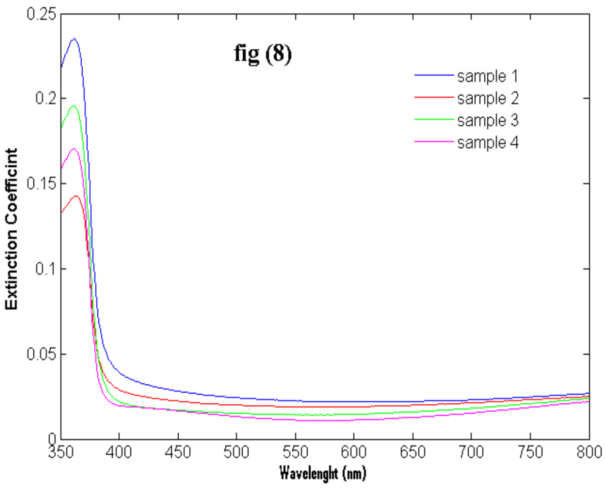

Fig. 8: The dependence of the extinction coefficient of the annealed films on the wavelength.

3.4. Magnetic properties

Magnetic Force Microscopy (MFM) is a special technique developed for the study of the magnetic materials and phenomena or to image a spatial distribution of a magnetic field. Usual samples for MFM can be magnetic tapes, hard disks and magneto-optical disks. When MFM measurements are performed, the tip shouldn’t come into the mechanical contact with the surface. The influence of the mechanical contact is usually stronger. Therefore during MFM the tip is scanned at a defined distance above the sample. This type of scanning is said the non-contact MFM.

The MFM of all samples was done in the room temperature. All images showed the magnetic property in the room temperature. Fig. 9 shows the MFM picture of sample 1. The Left image is the surface topography and the right image is 3D topography for sample 4 that it has been fitted by polynomial fit. The scanned surface is 1.5 µm × 1.5 µm. Domain is formed in MFM pattern. The degree of magnetization of each domain, however, is governed by the temperature of the material. The overall magnetization of the material is the vector sum of all magnetizations of the various domains. When the domains are magnetized in the same direction, they reinforce each other and thus giving a large magnetic field. Such a reinforce can be achieved by the action of a weak external magnetic field. Each domain is separated with others domains by a wall. The domain wall may be an abrupt boundary or gradual boundary that is strongly moved by external magnetic field.

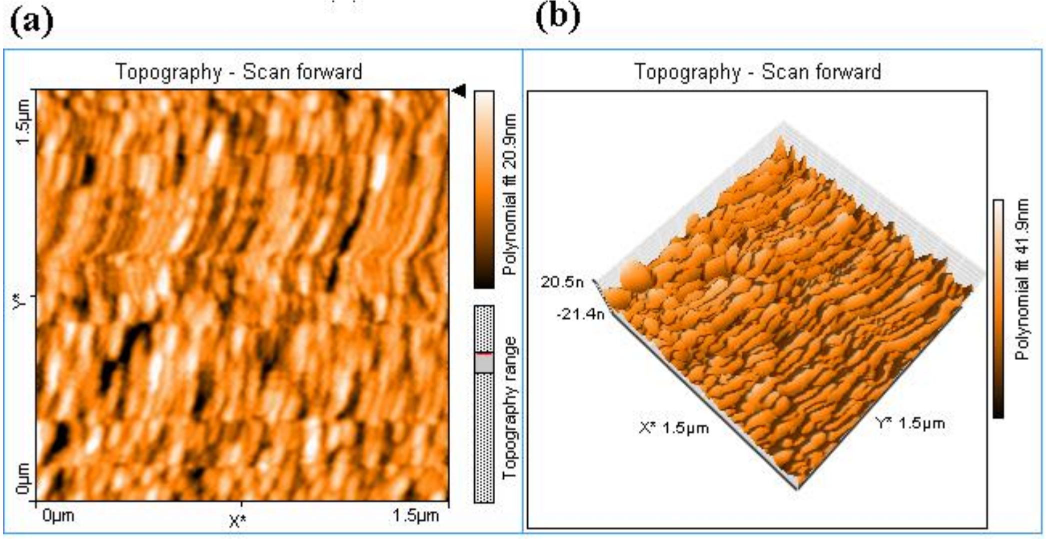

Fig. 9. The MFM image of sample 1 in room temperature. Left and right panel are 2D and 3D surface topography, respectively.

After observing the ferromagnetic MFM picture of the sample 1 in the room temperature, the hysteresis curve was measured and Fig. 10 shows it (M vs. H)). The saturation magnetization (M_s) up to 2000 Oe, the spontaneous magnetization (M_r) and the coercive magnetic field (H_C) were listed in table 2. The coercive magnetic field of all samples is almost the same and with the dispensable changes. Whatever the grain size is smaller, the saturated and spontaneous magnetization will be larger. This experiential work shows that the magnetic property of samples depends on grain size. Why the magnetic property of samples depends on grain size can be an open problem. Perhaps, one of reasons is the located carrier (electron/hole) in smaller grain size and thus it produces the magnetic property base on Hubburd’s model. The other reason may refer to formation an oxygen vacancy in thermal annealing. Pure zinc oxide is a nonmagnetic metal oxide which generally shows the diamagnetic property. The observation of ferromagnetism in these samples is a puzzle. What is the origin of formation of moments in such systems? Perhaps, the origin of the moments was attributed to certain types of oxygen vacancies. As seen, pH of the solvent controls the grain size of samples. When pH of the solvent is decreased, the grain size becomes also smaller. The smaller grain size at the annealing temperature 500 ^{o}C produces more oxygen defects which create magnetic property in samples. These defects with decreasing pH of the solvent are increased. Thus our samples have magnetic property.

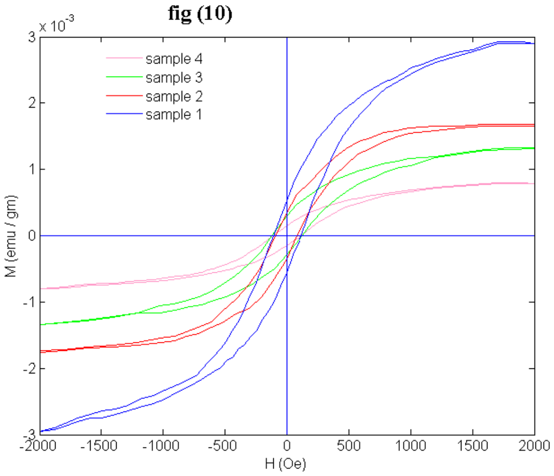

Fig. 10. Magnetization (M) versus magnetic field (H) curves for all samples at room temperature.

Table 2. The magnetic properties of samples

sample	magnetic property	magnetization (μemu/gm)		Coercive magnetic field(H_C) (Oe)
		Spontaneous (M_r)	saturation(M_s)	
1	ferromagnetism	0.534	2.893	102
2		0.357	1.673	95.35
3		0.301	1.327	102.7
4		0.146	0.789	102

4. Conclusion

This work has two aspects. Firstly, it shows that the sol gel method is a trustworthy technique for controlling grain size that can be performed by changing pH of the solvent. Secondly, it shows how with controlling the environmental parameters, the samples can produce not only inexpensive but also have unique physical properties especially the magnetic property without any doping.

Nano structures of materials are noticeable in the electronic and spintronic due to low consumption and high efficiency at industry. One of these materials is zinc oxide. Growth technique and environmental parameters are two very important factors for changing the physical properties of zinc oxide. In this work, four samples with the different pH were grown. EDX, AFM, XRD, MFM and PL characterizations were done on samples. The XRD spectrum of every sample corresponds to the hexagonal wurtzite structure. The crystalline quality is decreased with decreasing pH of the solvent. The AFM images of the annealed ZnO nano films with various grain sizes were performed in the room temperature. The calculations show that the root mean square roughness has a directly relation with pH of solvent. The smaller RMS is, the less pH of solvent will be. The drying and annealing transmittance spectrum of samples in room temperature illustrate that whatever grain size becomes smaller, the transmittance spectrum will decrease. The band gap calculations exhibited whatever the smaller the grain size is, the bigger the band gap energy will be because of quantum confinement effect. Three parameters of position, width and intensity of peak for each photoluminescence spectrum were studied. The peak position of each sample shows that the type of the recombination mechanism is free exciton (FE). The full width half maximum (FWHM) of all spectra was calculated that is decreased with decreasing the grain size or pH of the solvent and the light emission is also shifted to monochromatic light. The intensity of the photoluminescence spectrum shows that is subtracted with increasing grain size. The done magnetic property of all samples in the room temperature showed that all are ferromagnetism. Perhaps, one of reasons is the located carrier (electron/hole) in smaller grain size or the formation of the oxygen vacancy defects in the annealing temperature and thus it produces the magnetic property.

Acknowledgment

The authors would like to thanks Islamic Azad University, Varamin-Pishva Branch, for financial support of this research work.

References

[1] M Hosseinifard, L Hashemi, V Amani, A Morsali Journal of Structural Chemistry, **54**(2), 396 (2013).
[2] M. Yuonesi, A.Pakdel, Physica B, **405** 2083 (2010).
[3] A. Bera, D. Basak Chemical Physics Letters, **476**, 262 (2009).
[4] Wang Lguo, Zhang Pelling, J. Optoelectron. Adv. Mater., **16**(3-4), 300 (2014).
[5] M. Yuonesi, M. Izadifard, M. E. Ghazi, F. E. Ghodsi, Chinese Journal of Physics, **49**(4), 941 (2011).
[6] Paul Fons, Alexander V. Kolobov, Junji Tominaga, Berngere Hyot, Bernard Andre, J. Optoelectron. Adv. Mater., **16**(1-2), 1 (2014).
[7] J. B. Yi, H. Pan, J. Y. Lin, J. Ding, Y. P. Feng, S. Thongmee, T. Liu, H. Gong, L. Wang, Adv. Mater, **20,** 1170 (2008)
[8] Amritpal Singh, Praveen Kumar, J. Optoelectron. Adv. Mater. **16**(3- 4), 311 (2014).
[9] S. Shankar, M. Saroja, M. Venkatachalam, N. Muthukumarasamy, V. Kumar, International Journal of Innovative Research in Science, Engineering and Technology, **3**(2), 8990 (2014).
[10] M. Yuonesi, M. E. Ghazi, M. Izadifard, M. Yaghobi, J. Optoelectron. Adv. Mater. **10**(10), 2603 (2008).
[11] Hsin-Ming Cheng, Kuo-Feng Lin, Hsu-Cheng Hsu, Wen-Feng Hsieh, Applied Physics Lettters, **88**, 261909 (2006)
[12] Vladimir A. Fonoberov, Khan A. Alim, Alexander A. Balandin, Physical Review B, **73**, 165317 (2006)
[13] S. Mahanty, D. Basak, F. Rueda and M. Leon, Journal of Electronic Materials, **28**(5), 559 (1999)
[14] E G Birgin, I Chambouleyron, J M Martı´nez, J. Comput. Phys. **151**, 862 (1999)

---

[*] Corresponding author: hr_alaei@yahoo.com